Inflammasome Components Coordinate Autophagy and Pyroptosis as Macrophage Responses to Infection

Brenda G. Byrne,[a] Jean-Francois Dubuisson,[a]* Amrita D. Joshi,[a]* Jenny J. Persson,[b]* Michele S. Swanson[a]

Department of Microbiology and Immunology, University of Michigan Medical School, Ann Arbor, Michigan, USA[a]; Department of Molecular and Cellular Biology, Life Sciences Addition, University of California-Berkeley, Berkeley, California, USA[b]

* Present address: Jean-Francois Dubuisson, Flamel Technologies, Lyon, France; Amrita D. Joshi, Vascular Surgery Section, University of Michigan Medical School, Ann Arbor, Michigan, USA; Jenny J. Persson, Lund University, Lund, Sweden.

ABSTRACT When microbes contaminate the macrophage cytoplasm, leukocytes undergo a proinflammatory death that is initiated by nucleotide-binding-domain-, leucine-rich-repeat-containing proteins (NLR proteins) that bind and activate caspase-1. We report that these inflammasome components also regulate autophagy, a vesicular pathway to eliminate cytosolic debris. In response to infection with flagellate *Legionella pneumophila*, C57BL/6J mouse macrophages equipped with caspase-1 and the NLR proteins NAIP5 and NLRC4 stimulated autophagosome turnover. A second trigger of inflammasome assembly, K^+ efflux, also rapidly activated autophagy in macrophages that produced caspase-1. Autophagy protects infected macrophages from pyroptosis, since caspase-1-dependent cell death occurred more frequently when autophagy was dampened pharmacologically by either 3-methyladenine or an inhibitor of the Atg4 protease. Accordingly, in addition to coordinating pyroptosis, both (pro-) caspase-1 protein and NLR components of inflammasomes equip macrophages to recruit autophagy, a disposal pathway that raises the threshold of contaminants necessary to trigger proinflammatory leukocyte death.

IMPORTANCE An exciting development in the innate-immunity field is the recognition that macrophages enlist autophagy to protect their cytoplasm from infection. Nutrient deprivation has long been known to induce autophagy; how infection triggers this disposal pathway is an active area of research. Autophagy is encountered by many of the intracellular pathogens that are known to trigger pyroptosis, an inflammatory cell death initiated when nucleotide-binding-domain-, leucine-rich-repeat-containing proteins (NLR proteins) activate caspase-1 within inflammasome complexes. Therefore, we tested the hypothesis that NLR proteins and caspase-1 also coordinate autophagy as a barrier to cytosolic infection. By exploiting classical bacterial and mouse genetics and kinetic assays of autophagy, we demonstrate for the first time that, when confronted with cytosolic contamination, primary mouse macrophages rely not only on the NLR proteins NAIP5 and NLRC4 but also on (pro-)caspase-1 protein to mount a rapid autophagic response that wards off proinflammatory cell death.

Received 22 December 2012 **Accepted** 7 January 2013 **Published** 12 February 2013

Citation Byrne BG, Dubuisson J-F, Joshi AD, Persson JJ, Swanson MS. 2013. Inflammasome components coordinate autophagy and pyroptosis as macrophage responses to infection. mBio 4(1):e00620-12. doi:10.1128/mBio.00620-12.

Editor Arturo Zychlinsky, Max Planck Institute for Infection Biology

Address correspondence to Michele S. Swanson, mswanson@umich.edu.

In settings as diverse as HIV-infected T lymphocytes, infected plant leaves, fruit fly ovaries, and embryonic mouse lungs, autophagy is coupled to programmed cell death, as either a partner or an antagonist (1–4). Several intracellular bacterial pathogens that trigger the proinflammatory cell death known as pyroptosis (5) also stimulate autophagy, a mechanism to capture and eliminate cytoplasmic debris. To investigate how these two mechanisms of innate immunity are coordinated, we exploit *Legionella pneumophila*, a Gram-negative pathogen of water and soil amoebae that can also replicate within alveolar macrophages to cause the pneumonia Legionnaires' disease.

Unlike humans, mice and their macrophages are equipped to restrict *L. pneumophila* infection by processes coordinated by the nucleotide-binding-domain-, leucine-rich-repeat-containing proteins (NLRs) NAIP5 and NLRC4 (IPAF) and the cysteine protease caspase-1 (6–8). In particular, bacterial flagellin that contaminates the macrophage cytosol during type IV secretion is detected by NAIP5 (9–11), which then binds to NLRC4 (6). As a consequence, NLRC4 and pro-caspase-1 interact through their respective CARD domains to assemble an inflammasome complex, wherein the protease is activated. Caspase-1 cleaves pro-interleukin 1β (pro-IL-1β) and -IL-18 and also generates pores in the macrophage plasma membrane, thereby triggering osmotic lysis and release of mature proinflammatory cytokines (5, 12, 13). Thus, pyroptosis promotes inflammation while denying the pathogen its intracellular niche. In addition to coordinating pyroptosis, NAIP5, NLRC4, and caspase-1 limit the capacity of flagellate *L. pneumophila* to establish replication vacuoles by a mechanism that had not been elucidated (8, 14–18).

One barrier to infection that has been associated with inflammasome function is autophagy. This broadly conserved membrane traffic pathway can capture and degrade cytoplasmic material, such as damaged or redundant organelles (19). Autophagy can also function as an alternative mechanism for egress of a va-

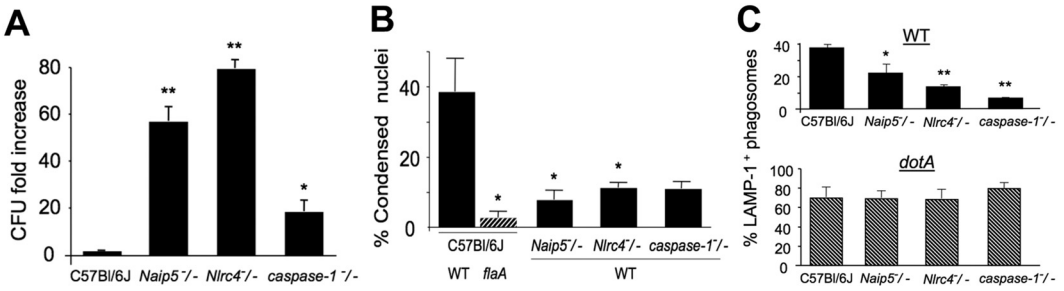

FIG 1 Inflammasome components in mouse macrophages restrict growth of *L. pneumophila*, coordinate pyroptosis, and alter bacterial trafficking. (A) NAIP5, NLRC4, and caspase-l equip mouse bone marrow-derived macrophages to restrict replication of flagellate *L. pneumophila*. Shown is the mean (± SD) fold increase in CFU from 2 to 72 h calculated from two experiments performed in duplicate after infection of cells of the genotypes indicated at an MOI of <1. **, $P < 0.01$; *, $P < 0.05$ compared to the C57BL/6J yield. (B) NAIP5, NLRC4 and caspase-1 equip macrophages to commit pyroptosis in response to flagellate *L. pneumophila*. The mean (± standard error [SE]) percentage of macrophages whose nucleus was round and phase dense, a morphological hallmark of pyroptosis, was calculated by scoring at least 100 macrophages 7 h after infection at an MOI of <1 with either WT or *flaA* mutant *L. pneumophila* in each of two (*flaA*) or more (WT) experiments. *, $P < 0.05$ compared to C57BL/6J cells infected with WT bacteria. (C) NAIP5, NLRC4 and caspase-1 promote delivery of *L. pneumophila* to the macrophage endosomal pathway. The mean (± SE) percentage of bacteria that colocalized with the late endosomal and lysosomal protein LAMP-1 was calculated by scoring at least 50 WT (top) or *dotA* mutant (bottom) intracellular bacteria 1.5 h after infection of macrophages of the genotype indicated at an MOI of <1 in two (*caspase-1*) or three (C57BL/6J, *Naip5*$^{-/-}$, and *Nlrc4*$^{-/-}$) independent experiments. **, $P < 0.01$; *, $P < 0.05$, compared to C57BL/6J cells.

riety of substrates, including the yeast protein Acb1, poliovirus, *Escherichia coli*, *Brucella abortus*, and proinflammatory cytokines (20–25). Both autophagy and inflammation are regulated by one class of NLR proteins that function independently of caspase-1. Molecular genetic studies of Crohn's inflammatory bowel disease revealed that NOD1 and NOD2, sensors of cytosolic peptidoglycan, not only induce autophagy by interacting directly with Atg16L1 but also regulate cytokine production via the NF-κB pathway (26, 27).

Also linked to autophagy is a second class of NLR proteins—those that collaborate with caspase-1 to initiate pyroptosis. Remnants of phagosomes ruptured by *Shigella flexneri* in host epithelial cells are decorated by components of both the autophagy and inflammasome machineries (28). Excess autophagosomes accumulate when *caspase-1*$^{-/-}$ mutant macrophages are infected by *S. flexneri* (29), indicating that caspase-1 may affect either autophagosome formation or maturation. Autophagosome maturation is sluggish in macrophages of A/J mice, whose partial loss-of-function NLR *Naip5* allele confers susceptibility to *L. pneumophila* (30). Moreover, in resting cells, NLRP4 and NLRC4 are complexed with Beclin-1/Atg6 (31), an early component of the autophagy pathway. Accordingly, an intriguing possibility is that microbe-associated microbial patterns (MAMPs) that stimulate inflammasome assembly simultaneously relieve NLR inhibition of Beclin-1 to induce autophagy. Moreover, recent molecular genetic studies demonstrated that stimulation of the AIM2 or NLRP3 inflammasome pathways also increases autophagy, which in turn targets the NLR proteins for disposal (32). Therefore, to investigate the ability of macrophage inflammasome components to modulate autophagy and pyroptosis as barriers to infection, we exploited an intracellular infection model that is amenable to genetic, kinetic, and dosage analysis.

RESULTS

Inflammasome components equip macrophages to alter *L. pneumophila* trafficking. We first verified that C57BL/6 mouse macrophages restrict replication by *L. pneumophila* by relying on NAIP5, NLRC4, and caspase-1 to recognize cytosolic flagellin and induce pyroptosis (7, 8). Compared to infected wild-type (WT) cells, macrophages that lacked each inflammasome component had a higher yield of viable bacteria (Fig. 1A) and lower frequency of pyroptotic nuclei (Fig. 1B).

In addition to caspase-1-dependent cell death, mouse macrophages limit replication vacuole formation by flagellate *L. pneumophila* by another mechanism that has not been defined (8, 14, 16–18). To verify this observation in our experimental system, WT and mutant C57BL/6J macrophages were first infected for 1.5 h with a bacterial dose too low to induce pyroptosis, and then delivery of virulent bacteria to LAMP-1$^+$ compartments was quantified. Indeed, resistant macrophages more frequently contained bacteria in LAMP-1$^+$ vacuoles than did cells from *Naip5*$^{-/-}$, *Nlrc4*$^{-/-}$, or *caspase-1*$^{-/-}$ mutant mice (Fig. 1C). The trafficking defect of each inflammasome-component mutant cell was specific to virulent *L. pneumophila*, since both resistant and permissive macrophages efficiently delivered avirulent *dotA* type IV secretion mutant bacteria to nonpermissive LAMP$^+$ vacuoles (Fig. 1C).

In resistant macrophages, a subset of *L. pneumophila* organisms do form replication vacuoles, but these compartments are later disrupted (8). To determine whether flagellin recognition by NAIP5 and NLRC4 contributes to lysis of pathogen replication vacuoles, we recorded whether progeny bacteria were vacuolar or dispersed in wild-type (WT) and mutant macrophages. After infection for 18 h, replication vacuoles were disrupted more frequently when the pathogens expressed flagellin and the macrophages produced NAIP5 and NLRC4 (Fig. 2A and B). By 40 h, *flaA* mutant *L. pneumophila* organisms had lysed the primary host cell and established secondary infections (8) (data not shown). In contrast, WT *L. pneumophila* organisms were degraded and scattered throughout the cell (Fig. 2A), consistent with the decline in the yield of CFU in resistant macrophages observed in this period (8, 15, 17). The multiple scattered and degraded bacteria likely represent the progeny of a single infectious bacterium, since at 2 h after infection, only ~10% of macrophages were infected, virtually all of these contained a single bacterium, and secondary infections are not typically observed until >18 h of infection. Therefore, in

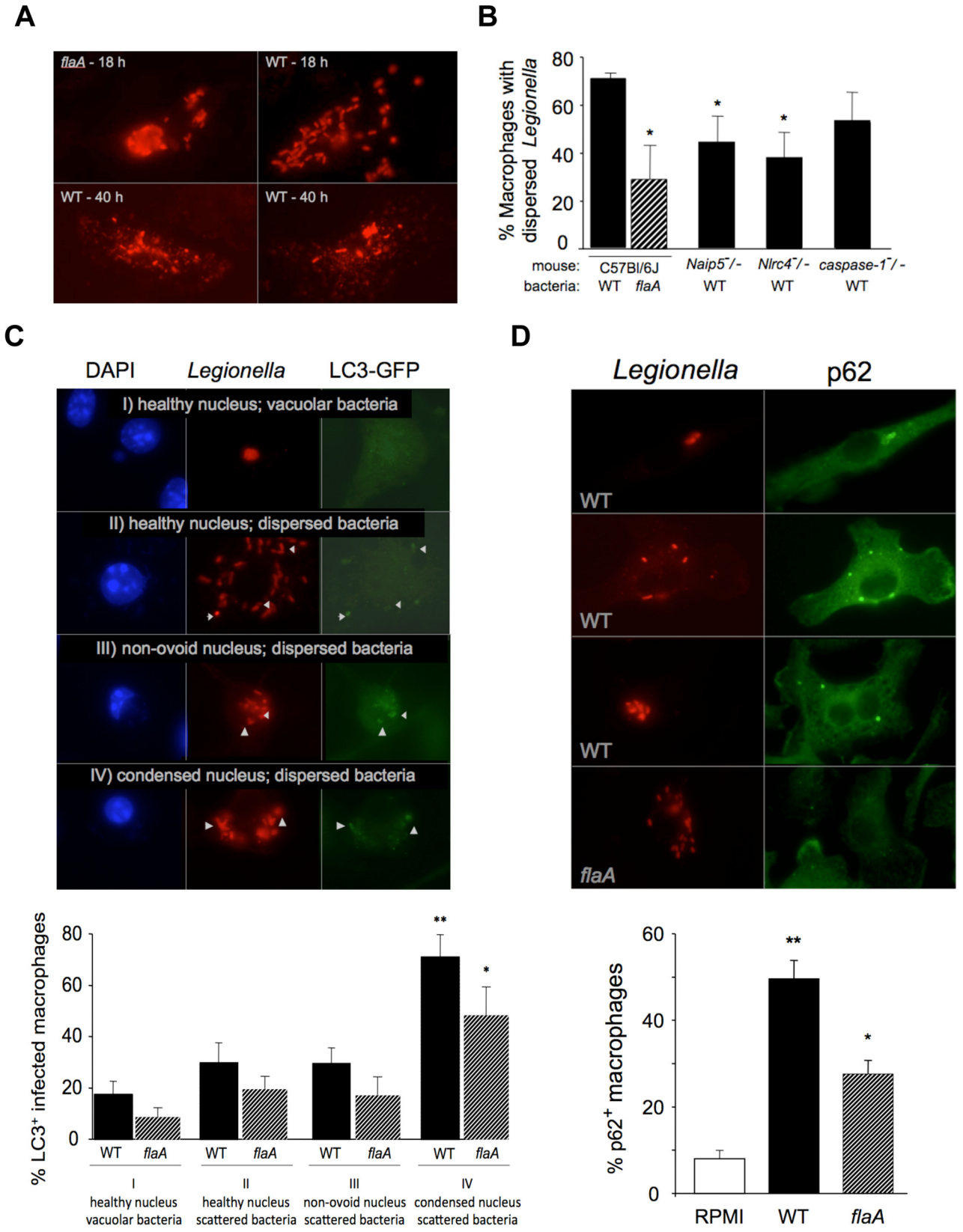

FIG 2 Inflammasome components equip macrophages to disrupt *L. pneumophila* replication vacuoles, which correlates with autophagy. (A) After infection of C57BL/6J macrophages with WT or *flaA* mutant *L. pneumophila* at an MOI of <1 for 18 or 40 h, bacteria (red) were vacuolar (*flaA*-18h), dispersed rods (WT-18h) or degraded (WT-40 h). (B) The mean (± SE) percentage of macrophages containing dispersed WT or *flaA* mutant bacteria 18 h after infection was

(Continued)

addition to contributing to pyroptosis, the NLR proteins NAIP5 and NLRC4 equip mouse macrophages to perturb not only the immediate trafficking of *L. pneumophila* but also the stability of mature replication vacuoles.

Since intracellular pathogens that perforate their vacuoles induce autophagy (33–35), we investigated whether resistant macrophages activated this degradation pathway. Macrophages were infected at a multiplicity of infection (MOI) of <1 for 13 h, a time point after bacterial replication has begun but before either secondary infections or detachment of pyroptotic cells. To analyze these asynchronous infections, autophagy was quantified by counting puncta of GFP-LC3 and p62, and the macrophage response to infection was categorized according to the morphologies of the cell, bacterial vacuole, and nucleus. Macrophages that were still well spread and that contained bacteria within replication vacuoles rarely had LC3 puncta (Fig. 2C, category I). Conversely, GFP-LC3 frequently colocalized with dispersed *L. pneumophila* in macrophages that had already committed pyroptosis, identified as rounded cells with condensed nuclei category IV. Dispersal of the bacteria also correlated with the appearance of puncta of p62 (Fig. 2D), a protein that links LC3 to ubiquitinated substrates (36, 37). Autophagy may precede pyroptosis, since GFP-LC3 puncta were also evident in some healthy macrophages that contained dispersed bacteria (Fig. 2C, category II). However, these trends did not reach statistical significance, perhaps because the 13-h infection was asynchronous and membrane-bound LC3 is short-lived due to efficient degradation within autophagolysosomes (37, 38).

To gauge the contribution of flagellin to the macrophage autophagy and pyroptosis response to dispersed bacteria, we quantified the autophagy markers LC3 and p62 in resistant macrophages infected with WT or *flaA* mutant *L. pneumophila*. Compared to cells infected with WT pathogens, LC3 and p62 puncta were present less frequently in macrophages that contained scattered *flaA* mutant bacteria (Fig. 2C and D). Thus, flagellin is one of multiple stimulatory factors released by *L. pneumophila*. A similar scenario was reported to occur when replicating *L. pneumophila sdhA* mutants are released from their unstable vacuoles in permissive A/J *Naip5* mutant macrophages (35). Independently of flagellin recognition, LC3 colocalizes with some scattered bacteria, many are degraded, and pyroptosis is induced (35). A residual flagellin-independent response to replicating *L. pneumophila* is expected, since flagellin expression is not detected in replicating *L. pneumophila* (39), microbe-associated microbial patterns (MAMP) of *L. pneumophila* other than flagellin activate inflammasomes (35, 40), and *flaA* mutant *L. pneumophila* are eventually cleared from the lungs of C57BL/6J mice (8).

This series of morphological and genetic studies indicated that, in addition to pyroptosis (Fig. 1B and 2C), the bacterial MAMP flagellin and the mouse NLR proteins NAIP5 and NLRC4 potentiate two other responses by resistant macrophages: disruption of the *L. pneumophila* replication vacuole (Fig. 2A and B) and autophagy (Fig. 2C and D). Therefore, we next applied a more rigorous genetic test of whether inflammasome components impact the autophagy response.

Inflammasome components stimulate autophagosome turnover. To investigate whether NAIP5, NLRC4, and caspase-1 equip macrophages to stimulate the autophagy pathway in response to cytosolic flagellin, we applied a pulse-chase method developed previously (38). Because LC3$^+$ autophagosomes have a half-life of <30 min in primary C57BL/6J mouse macrophages (38), we increased the sensitivity of our cell biological assays by examining the impact of short, synchronous infections on a large population of preformed autophagosomes.

When transferred to amino acid-free buffer for 20 min, C57BL/6J mouse macrophages rapidly accumulate multiple vacuoles decorated by LC3 (Fig. 3A and B) and lipidated LC3 protein (38) (data not shown), a second indicator of autophagy (37). When C57BL/6J macrophages that contained numerous preformed autophagosomes were then exposed to virulent *L. pneumophila*, the number of LC3$^+$ vacuoles diminished to baseline within 10 min (Fig. 3A and B). In contrast, in uninfected C57BL/6J macrophages, autophagosome maturation typically requires 30 min, as determined by analyzing the size of the LC3$^+$ vacuole population and the amount of lipidated LC3 protein after the macrophage amino acid supply has been restored (38). When fusion of autophagosomes with lysosomes was inhibited by pretreating macrophages with bafilomycin A (37), the size of the LC3$^+$ vacuole population increased in uninfected macrophages but still declined rapidly in response to *L. pneumophila* (Fig. 3C). Therefore, rather than stimulating autophagosome maturation, flagellin recognition by inflammasome components may stimulate autophagosome egress (20–25).

Rapid turnover of autophagosomes was coordinated by the inflammasome components that respond to cytosolic flagellin. First, the number of LC3$^+$ vacuoles was stable in resistant macrophages infected with *flaA* flagellin or *dotA* secretion mutants (Fig. 3A and B). Second, the size of the LC3$^+$ vesicle population remained stable when *Nlrc4*$^{-/-}$ or *caspase-1*$^{-/-}$ mutant macrophages were infected with either WT, *flaA*, or *dotA L. pneumophila* (Fig. 3B). Third, NAIP5 also contributed, since macrophages that lacked this NLR did not exhibit a rapid decline in autophagosome number in response to flagellate, type IV secretion-competent *L. pneumophila* (Fig. 3B). The modest decline in vacuoles observed in *Naip5*$^{-/-}$ macrophages was neither dependent on flagellin nor statistically significant. A fourth striking observation was that, compared to C57BL/6J, *Naip5*$^{-/-}$, and *Nlrc4*$^{-/-}$cells, macrophages obtained from caspase-1$^{-/-}$ mutant mice harbored significantly fewer autophagosomes 20 to 30 min after transfer to amino acid-free buffer (Fig. 3B and D). Together, these results indicate that inflammasome components, including (pro-)caspase-1 protein, equip macrophages to stimulate rapid autophagosome turn-

Figure Legend Continued

calculated for >100 infected macrophages of the genotypes indicated in three (WT) or two (*flaA*) experiments. *, $P < 0.05$ compared to C57BL/6J cells infected with WT bacteria. (C) After infection of macrophages from transgenic LC3-GFP C57BL/6J mice for 13 h with WT or *flaA* mutant *Legionella* (red) at an MOI of <1, the mean % (± SE) of macrophages of each of four morphological classes (blue nuclei) that contained at least 3 LC3-GFP+ puncta (green) was calculated by scoring >200 macrophages in each of four experiments. **, $P < 0.01$ and *, $P < 0.05$, compared to macrophages with normal nuclei and vacuolar bacteria. Arrows indicate LC3 colocalization with bacteria. (D) After infecting C57BL/6J macrophages for 13 h with WT or *flaA* mutant *L. pneumophila* at an MOI of <1, the mean (± SE) % uninfected (RPMI) or infected macrophages (red) containing two or more p62 puncta (green) was calculated by scoring at least 100 macrophages in three (RPMI) or four (WT, *flaA*) independent experiments. **, $P < 0.01$ and *, $P < 0.05$ compared to uninfected macrophages.

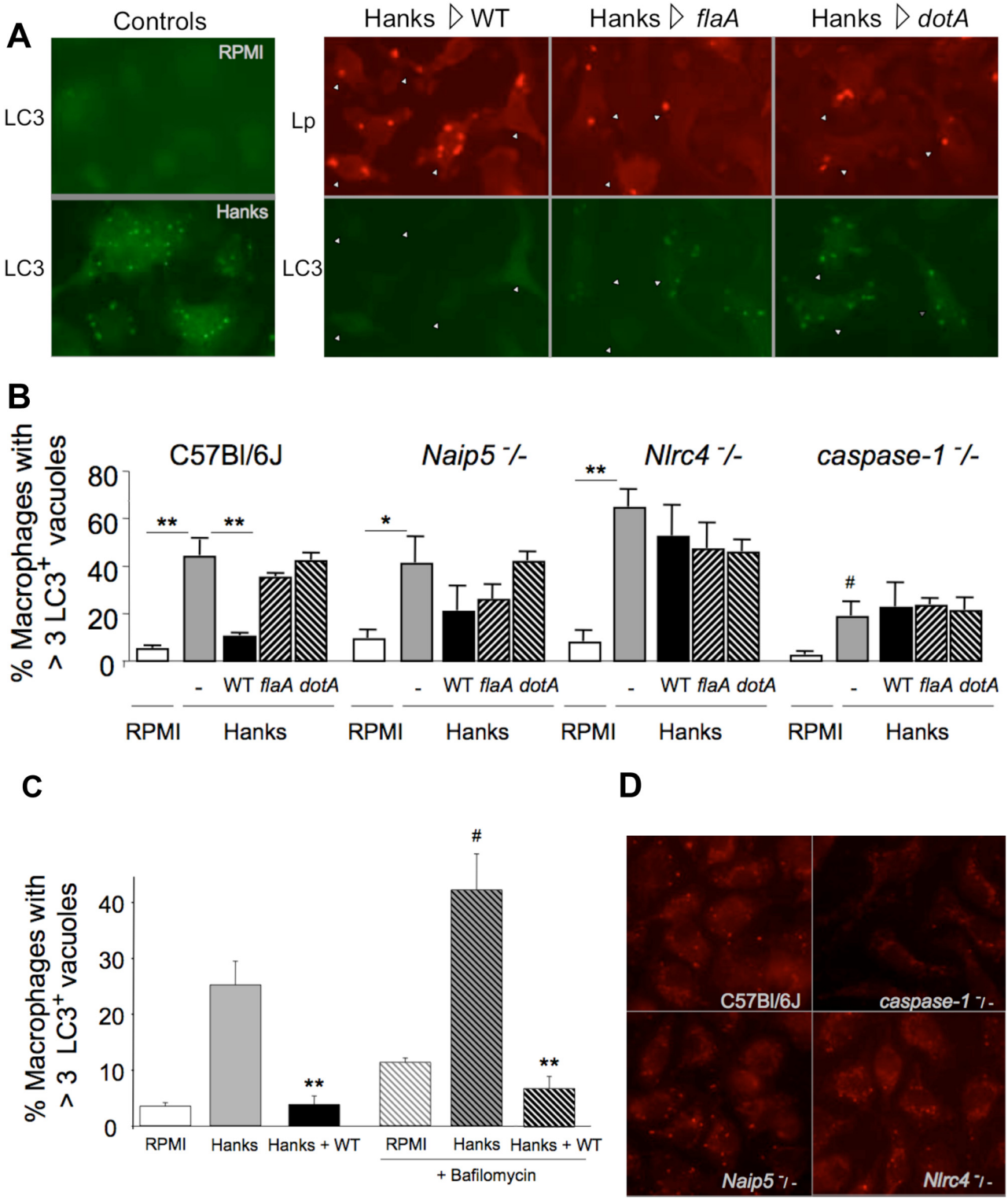

FIG 3 Inflammasome components promote rapid autophagosome flux in response to flagellate, type IV secretion-competent *L. pneumophila*. (A) Transgenic GFP-LC3 C57BL/6J macrophages were maintained in RPMI or treated for 20 min with Hanks buffer before identifying autophagosomes using GFP-specific antibody (LC3). Alternatively, after a population of autophagosomes had been generated, macrophages were infected for 10 min with WT, *flaA*, or *dotA* mutant *L. pneumophila* at an MOI of 3 (WT, *dotA*) or <10 (*flaA*) before immunolabeling of bacteria (Lp) and autophagosomes (LC3). Arrowheads indicate infected macrophages. (B) Macrophages of the indicated genotypes were treated as described above to calculate the mean (± SE) percentage of 100 macrophages containing >3 autophagosomes labeled with LC3-specific antibody in each of three experiments. **, $P < 0.01$; *, $P = 0.05$, compared to Hanks buffer-treated cells; #, $P = 0.04$ compared to C57BL/6J macrophages treated with Hanks buffer. (C) C57BL/6 transgenic GFP-LC3 macrophages were incubated for 30 min with or without 25 nM bafilomycin A, an inhibitor of autophagosome-lysosome fusion, treated for 20 min with Hanks buffer with or without bafilomycin A, and then

(Continued)

over as a response to cytosolic stress, such as exposure to the MAMP flagellin.

Caspase-1 promotes autophagy in response to K^+ efflux. As an independent test of the contribution of caspase-1 protein to autophagy, we exploited the observation that efflux of cytosolic K^+ mediated by ionophores induces inflammasome assembly (41). Treatment of microglial cells or macrophages with ATP, a ligand of the P2X7 receptor that induces K^+ efflux, is known to stimulate autophagosome accumulation and egress (23, 42), but whether caspase-1 contributed was not investigated. THP-1 monocytic cells and primary mouse macrophages do accumulate activated LC3 in the presence or absence of caspase-1 protein when the NLRP3 or AIM2 inflammasome pathway is stimulated by prolonged treatment with the K^+ ionophore nigericin or transfected double-stranded DNA (32).

Exposure of macrophages for 1 h to the K^+ ionophore valinomycin at either 50 or 100 μM was not sufficient to induce appreciable caspase-1 activation (Fig. 4A) or pyroptosis (data not shown). In contrast, treatment with as little as 10 to 50 μM valinomycin stimulated accumulation of $LC3^+$ vacuoles (Fig. 4B and C). Autophagy accounted for these puncta, since lipidated LC3 protein also accumulated in macrophages within 30 min of exposure to 100 μM valinomycin (Fig. 4D). Efflux of cytosolic K^+ was required for the autophagy response to valinomycin, since supplementation of the culture medium with 150 mM KCl abrogated the accumulation of both $LC3^+$ vacuoles and lipidated LC3 in treated cells (Fig. 4B to D).

To investigate whether activity of the caspase-1 protease contributes to the autophagy response, macrophages were treated with the caspase-1 peptide inhibitor ac-YVAD-cmk (100 μM; Alexis Biochemicals) for 1 h before exposure to valinomycin. Under these conditions, the autophagy response to K^+ efflux was not significantly different from that of cells with full caspase-1 activity (Fig. 4C and D). In contrast, the same ac-YVAD-cmk pretreatment protected macrophages from pyroptosis stimulated by flagellate *L. pneumophila*, as judged by quantifying condensed nuclei and lactate dehydrogenase (LDH) release (Fig. 4E). Therefore, in response to K^+ efflux, pyroptosis requires caspase-1 activity, yet macrophages require little or no caspase-1 protease activity to induce autophagy.

To test whether macrophages require (pro-)caspase-1 protein to stimulate autophagy in response to efflux of cytosolic K^+, the rate of LC3 lipidation by WT and mutant cells was analyzed. Compared to C57BL/6J macrophages, cells that lacked pro-caspase-1 protein consistently accumulated significantly less activated LC3 protein 20 and 40 min after treatment with the K^+ ionophore (Fig. 4F). Likewise, after a 1-h treatment with valinomycin, the number of caspase-1 mutant macrophages that contained >3 $LC3^+$ puncta was $>50\%$ lower than the number of WT cells (>100 cells in each of three experiments). Thus, amino acid withdrawal (Fig. 3B and D), flagellate and type IV secretion-competent *L. pneumophila* (Fig. 3B), and K^+ efflux (Fig. 4C, D, and F) each stimulated a rapid autophagy response by a mechanism that required relatively little or no caspase-1 enzyme activity but that was augmented by (pro-)caspase-1 protein, the scaffold for NLR assembly of inflammasome complexes.

Autophagy protects macrophages from pyroptosis induced by *L. pneumophila*. A cohort of inflammasome components equipped macrophages to induce both autophagy and pyroptosis in response either to flagellate *L. pneumophila* (Fig. 1 to 3) or K^+ efflux (Fig. 4). In each case, the stimulus and the caspase-1 protease activity sufficient to activate autophagy were lower than those required to induce pyroptosis (Fig. 2C and D and 4A to D), suggesting that inflammasome components can induce autophagy at early signs of danger. Therefore, we tested whether this vesicular disposal pathway increases the contamination threshold at which macrophages commit pyroptosis.

For this purpose, we applied a pharmacological inhibitor of the Atg4 cysteine protease. Compound NSC 377071 (50 μM) reduced the amount of both $LC3^+$ vacuoles (Fig. 5A) and activated LC3-II (Fig. 5B) that accumulated in Hanks buffer-treated macrophages, although not as completely as 3-methyladenine (3-MA), a nonspecific inhibitor of a class III phosphatidylinositol 3-kinases required for autophagy (37). Likewise, the Atg4 inhibitor reduced by ~60% the fraction of macrophages that contained >3 $LC3^+$ vacuoles 13 h after infection with WT *L. pneumophila* (Fig. 5C).

When autophagy was inhibited, macrophages underwent pyroptosis at twice the rate of untreated cells, as judged by scoring the fraction of infected cells whose nuclei were condensed (Fig. 5D). Likewise, infected macrophages also underwent pyroptosis more than twice as often when autophagy was inhibited with 3-MA (data not shown). We verified that macrophages with a condensed nucleus had a second hallmark of pyroptosis—a plasma membrane that was permeable to the DNA stain propidium iodide (PI) (5, 13). After macrophages had been infected for 2 h at three MOIs, every cell with a condensed nucleus was also PI^+ ($n > 200$ in each of two experiments). In contrast, PI was not retained by $>95\%$ of uninfected macrophages ($n > 200$) or macrophages that were infected but whose nucleus was not condensed ($n > 200$).

The increased sensitivity to flagellate *L. pneumophila* of macrophages treated with the Atg4 protease inhibitor was attributable to pyroptosis, since even heavily infected macrophages were completely protected from death by pretreatment with inhibitors of both Atg4 and caspase-1 (YVAD, 100 μM) (Fig. 5D). The more frequent death of cells treated with the Atg4 inhibitor was also a specific response to flagellin, since macrophages infected with >3 *flaA* mutant bacteria and uninfected cells each retained normal nuclear morphology in the presence or absence of the Atg4 inhibitor ($<2\%$ condensed nuclei in >200 macrophages scored for each of the four treatment groups in three independent experiments). Thus, in addition to coordinating pyroptosis, inflammasome components are poised to stimulate autophagy, a disposal pathway that raises the threshold of contaminants necessary to trigger proinflammatory cell death of macrophages.

Figure Legend Continued

incubated for an additional 15 min without or with *L. pneumophila* at an MOI of ~1. More than 100 macrophages were scored for the presence of >3 LC3 vacuoles localized using GFP-specific antibody. Means ($\pm$ SE) were calculated from four experiments. **, $P < 0.05$ compared with corresponding Hanks buffer-treated macrophages; #, $P < 0.01$ compared with macrophages treated with Hanks buffer but not bafilomycin A. (D) Macrophages of the genotypes shown were treated with Hanks buffer for 30 min, and then autophagosomes were visualized using LC3-specific antibody.

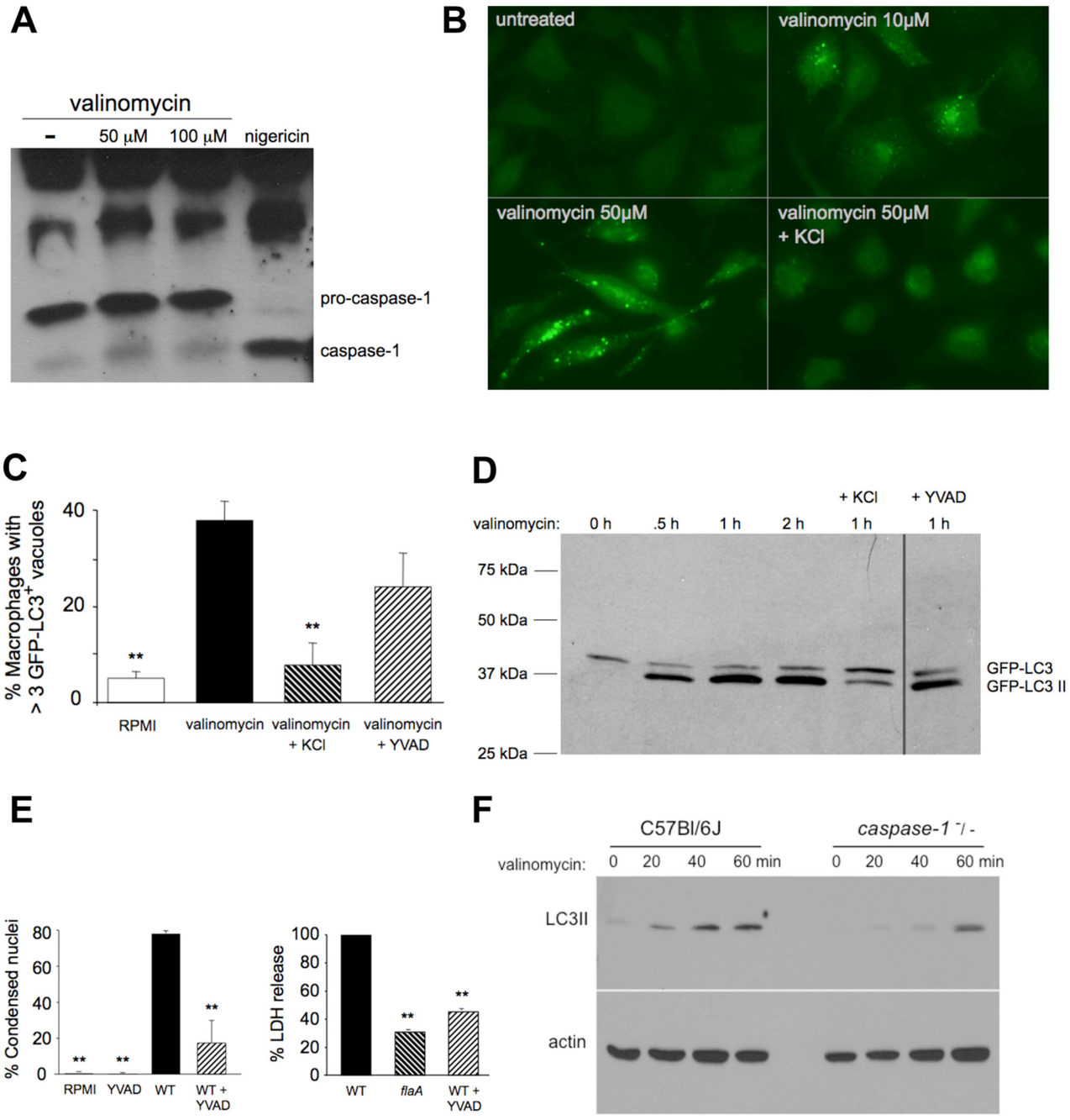

FIG 4 Caspase-1 promotes autophagy in response to K^+ efflux. (A) Caspase-1 cleavage by macrophages treated for 1 h with valinomycin or 2 h with 20 μM nigericin. Results are representative of two experiments. (B) GFP-LC3$^+$ autophagosomes of transgenic C57BL/6J macrophages maintained in RPMI or exposed 1 h to valinomycin with or without 150 mM KCl. (C) Mean (± SE) percentage of macrophages containing >3 GFP-LC3$^+$ vacuoles after 1 h with 50 μM valinomycin with or without 150 mM KCl and with or without 1 h pretreatment with 100 μM YVAD, a caspase-1 inhibitor, was calculated for >100 cells in each of >3 experiments. **, $P < 0.01$ compared to valinomycin-treated macrophages. (D) Lipidated GFP-LC3II in transgenic macrophages in RPMI or treated for 0.5 to 2 h with 100 μM valinomycin with or without KCl and with or without 1 h YVAD pretreatment. Similar results were obtained in three other experiments. (E) Pyroptosis by macrophages cultured for 1 h with or without 100 μM YVAD and incubated for 1 h without (RPMI) or with WT *L. pneumophila* at an MOI ~50 was measured as the mean percentage (± SD) of >100 macrophages whose nucleus was round and phase dense or as the percentage of LDH released from macrophages with or without YVAD pretreatment and 1 h incubation with WT or *flaA* mutant *L. pneumophila* at an MOI of ~25. The mean (± SD) percenage of LDH released in the absence of flagellin or presence of YVAD was calculated relative to LDH released after infection with WT bacteria calculated in two experiments. **, $P < 0.01$ compared infection with WT. (F) Lipidated LC3II and actin in macrophages of the genotypes shown treated for 0 to 60 min with 50 μM valinomycin. Similar results were obtained in three experiments.

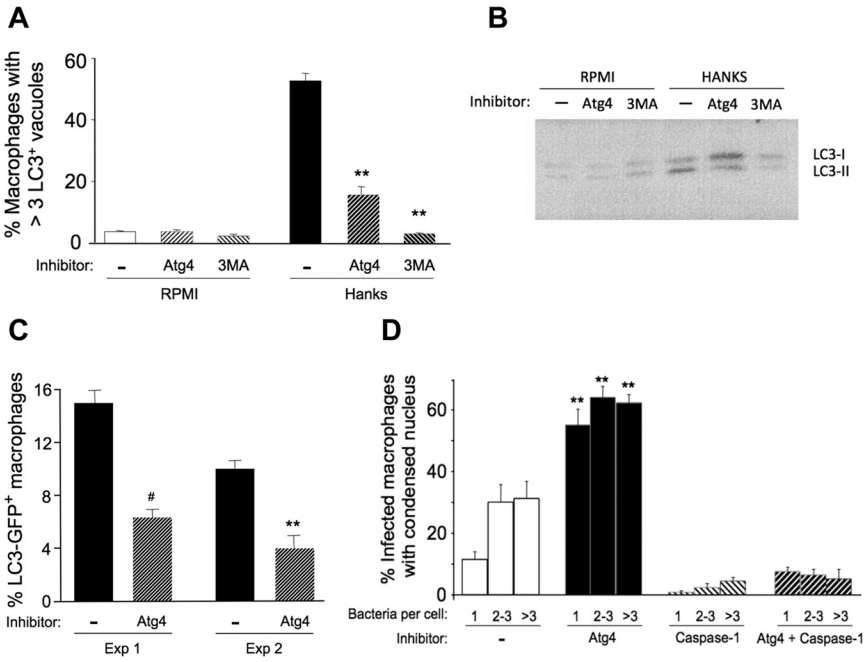

FIG 5 Autophagy protects macrophages from pyroptosis induced by *L. pneumophila*. (A) C57BL/6J macrophages cultured 1 h with or without 50 μM Atg4 inhibitor or 10 mM 3-MA were then incubated 35 min in rich medium (RPMI) or amino acid-free Hanks buffer with or without inhibitors before immunolocalization of autophagosomes. The mean fraction (± SE) of macrophages that contained >3 LC3 puncta was calculated by scoring >100 macrophages in each of two or three samples in two independent experiments. Similar results were obtained when the Atg4 inhibitor was analyzed in two other independent experiments that analyzed either endogenous LC3 or GFP-LC3. **, $P < 0.01$ compared to macrophages exposed only to Hanks buffer. (B) C57BL/6J macrophages cultured for 1 h with or without 50 μM Atg4 inhibitor or 10 mM 3-MA were then incubated 30 min in RPMI or Hanks buffer with or without inhibitors before analysis of endogenous LC3 protein. Similar patterns were observed in three other independent experiments. (C) After infecting macrophages from transgenic LC3-GFP C57BL/6J mice for 2 h with WT *Legionella*, cells were cultured for an additional 11 h with or without 50 μM Atg4 inhibitor before the mean percentage (± SE) of macrophages that contained at least 3 LC3-GFP+ puncta was calculated. In each of two experiments (Exp 1 and Exp 2), >100 total macrophages on 2 to 4 coverslips were scored. #, $P = 0.08$; **, $P < 0.01$, compared to infected but untreated cultures. (D) C57BL/6J macrophages cultured 1 h with or without inhibitors of Atg4 (50 μM) or caspase-1 (100 μM YVAD) were then infected with *L. pneumophila* with or without inhibitors for 2 h before cells were fixed and analyzed. The mean fraction (± SE) of macrophages containing the indicated number of bacteria whose nucleus was condensed was calculated by scoring >50 infected macrophages in each of 5 to 6 samples in one experiment. Similar results were obtained in three other independent experiments. **, $P < 0.01$ compared to macrophages that were untreated (RPMI) or treated with each or both inhibitors.

DISCUSSION

Our genetic and cell biological studies indicate that inflammasome components equip macrophages to calibrate their response to danger by recruiting either autophagy to dispose of cytosolic contaminants or pyroptosis to direct additional leukocytes to the task. Our working model (Fig. 6) considers mouse macrophage resistance to *L. pneumophila* infection in the context of recent molecular genetic studies of NLR proteins. In resting macrophages, NLRC4 binds the autophagy component Beclin-1/Atg6, inhibiting the autophagy pathway (31). When flagellin contaminates the cytoplasm during type IV secretion (6–8), NAIP5 binds both this MAMP (9–11) and NLRC4 (6, 43). The CARD domain of NLRC4 then promotes assembly of the flagellin-NAIP5-NLRC4 complex with pro-caspase-1, which we propose relieves NLRC4 repression of Beclin-1/Atg6 and induces autophagy. The autophagy disposal pathway then sequesters and disposes of contaminants, either by merging with lysosomes (19) or by delivering the cargo to the plasma membrane (21–25). We postulate that when the contaminants exceed the capacity of the autophagy disposal pathway, an increase in the number and/or stability of assembled inflammasomes activates sufficient caspase-1 to coordinate pyroptosis. Thus, as a consequence of more serious threats, infected cells undergo a programmed cell death that denies the pathogen its protected niche while stimulating an inflammatory response.

Caspase-1 appears to modulate autophagy by multiple direct or indirect mechanisms, some independent of its NLRC4 interaction or protease activity. Macrophages require the (pro-)caspase-1 protein to induce a rapid autophagy response not only to cytosolic flagellin (Fig. 3B) but also to nutrient withdrawal (Fig. 3B and D) or subphysiological levels of cytosolic K^+ (Fig. 4F). *Drosophila melanogaster* also requires a caspase protein, Dcp-1, to accumulate autophagosomes in response to amino acid starvation (44). Its capacity to interact with multiple NLR proteins (41) may equip pro-caspase-1 to modulate autophagy in response to a variety of stresses.

Rather than being absolutely required for macrophage autophagy, (pro-)caspase-1 confers a kinetic advantage. After starvation treatments of <0.5 h, *caspase-1*$^{-/-}$ macrophages contained fewer autophagosomes than did WT cells (Fig. 3B and D), whereas a 2-h incubation with amino acid-free buffer generated similar numbers of autophagosomes in WT and mutant macrophages (29). Likewise, *caspase-1*$^{-/-}$ macrophages appear to contain less activated LC3-II protein 1 h, but not 2 h, after induction of autophagy with sirolimus (rapamycin) (29). Unlike the differences observed at 40 min (Fig. 4F), after a 4-h treatment to induce K^+ efflux, the amount of lipidated LC3 was similar in macrophages that contain and those that lack caspase-1 protein (32).

Compared to pyroptosis, macrophage autophagy required little or no caspase-1 enzyme activity to respond to K^+ efflux (Fig. 4). Accordingly, autophagy may account for two previously described bacterial clearance processes that operate independently of caspase-1 enzyme activity. Mouse macrophages restrict *L. pneumophila* replication even when mature caspase-1 is not detectable by Western analysis (18). Also, caspase-1 protein promotes clearance of *Salmonella enterica* serovar Typhimurium from mice independently of its cleavage of IL-1β and IL-18 (45). Thus, by mechanisms that remain to be defined biochemically, (pro-)caspase-1 protein enables macrophages not only to activate proinflammatory cytokines and coordinate pyroptosis but also to induce a robust autophagy response.

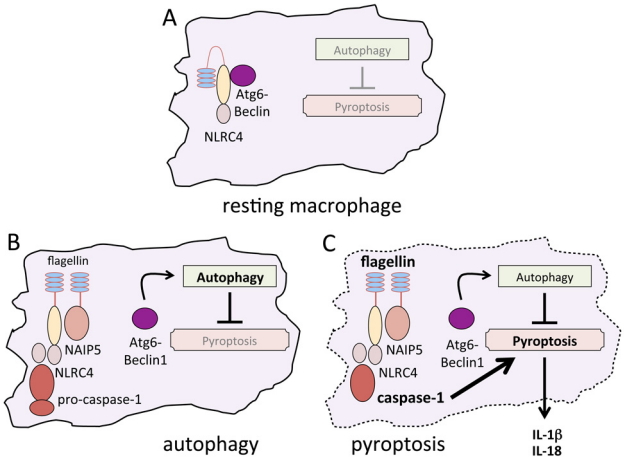

FIG 6 Model proposing how inflammasome components coordinate autophagy and pyroptosis as macrophage responses to infection. The following working model interprets cellular microbiology data presented here in the context of the current NLR literature cited in Discussion. (A) In resting macrophages, NLRC4 is complexed with autophagy component Beclin-1/Atg6, inhibiting autophagy. (B) In response to low levels of contamination, flagellin-bound NAIP5 recruits NLRC4 to a complex with pro-caspase-1 protein, derepressing autophagy, a cytoprotective disposal pathway. (C) When the capacity of autophagy to eliminate cytosolic contaminants is exceeded, an increase in the number and/or stability of inflammasome complexes activates sufficient caspase-1 to orchestrate pyroptosis, a programmed cell death that eliminates the pathogen's protected niche while initiating an inflammatory response.

In response to cytosolic flagellin, macrophages that encode caspase-1 and the NLR proteins NLRC4 and NAIP5 stimulated autophagosome turnover (Fig. 3). The fate of preformed $LC3^+$ vacuoles in infected cells remains to be determined, but several observations are consistent with the hypothesis that cytosolic MAMPs stimulate autophagosome egress. First, flagellate *L. pneumophila* still stimulated rapid $LC3^+$ turnover when autophagosome fusion with lysosomes was inhibited by bafilomycin A, a treatment sufficient to increase the size of the autophagosome population in control cells (Fig. 3C). Second, the autophagosomal pathway delivers a variety of microbes and proteins to the cell surface (21–25). Third, ATP, another trigger of K^+ efflux, induces egress of autophagosomal components from microglial cells (46) and rapid turnover of $LC3^+$ vacuoles in C57BL/6J macrophages (data not shown). Fusion of exosomes and lysosomes with the plasma membrane can also be stimulated by intracellular pathogens and inflammasome components (46–50). Finally, in uninfected primary mouse macrophages, measurable traffic of endogenous LC3 to the cell surface is evident within 20 min of withdrawal of amino acids, as judged by immunofluorescence microscopic analysis of cells that were fixed but not permeabilized (data not shown). Accordingly, a model that warrants testing is one in which macrophages exploit the autophagy pathway to capture and secrete not only proinflammatory cytokines (25) but also cytoplasmic microbial antigens, two mechanisms for stimulating neighboring leukocytes.

Autophagy protects macrophages infected with *L. pneumophila* against pyroptosis (Fig. 5), reinforcing the idea that this disposal pathway counteracts inflammation (19, 32, 51). By sequestering damaged mitochondria and limiting their production of reactive oxygen species, autophagy inhibits activation of NLRP3 inflammasomes, a cytosolic surveillance system that coordinates expression, maturation, or secretion of proinflammatory cytokines (52, 53). Furthermore, autophagy can capture and degrade pro-IL-1β and IL-18, limiting their secretion by macrophages and inflammatory responses in mice (54, 55). Indeed, in macrophages infected with *Shigella flexneri* or *Mycobacterium tuberculosis* or exposed to MAMPs, autophagy dampens production of IL-1β (29, 32, 56). Macrophages may also enlist autophagy to downregulate inflammasome signaling, since some NLR proteins are ubiquitinated and associated with p62 and Beclin-1 (32). Thus, by coupling autophagy with inflammasome function, macrophages can dictate whether to capture and eliminate cytosolic contaminants or instead to mount an inflammatory response.

The rapid mouse macrophage response to flagellate and type IV secretion competent *L. pneumophila* (Fig. 3) reinforces the paradigm that autophagy is a component of innate immunity (19). For example, compared to WT *Dictyostelium discoideum*, Atg9 mutant amoebae are more permissive for *L. pneumophila* infection (57). Likewise, the yield of *L. pneumophila* in A/J *Naip5* mutant mouse macrophages increases when expression of Atg5 is reduced by small interfering RNA (siRNA) (58). Conversely, when autophagy by A/J macrophages is induced with 2-deoxy-D-glucose, *L. pneumophila* replication is inhibited (58). *L. pneumophila* also retards maturation of its autophagosomal replication vacuole in permissive *Naip5* mutant A/J macrophages (30). A number of *L. pneumophila* Dot/Icm type IV secretion effectors manipulate the activity of multiple host GTPases that are known to contribute to autophagosome biogenesis (reviewed in reference 59), and the RavZ effector catalyzes deconjugation of LC3 from lipids and reduces the number of autophagosomes in infected cells (60). Thus, pathogens that persist within host cells can acquire mechanisms to subvert the autophagy pathway (61) and are excellent experimental tools to investigate how autophagy contributes to infection and immunity.

MATERIALS AND METHODS

Mice. Six- to eight-week-old female C57BL/6J mice were purchased from the Jackson Laboratory. A breeding pair of C57BL/6N mice expressing transgenic GFP-LC3 provided by Noboru Mizushima (37) (Tokyo Medical and Dental University, Tokyo, Japan) were housed in the University Laboratory Animal Medicine Facility at the University of Michigan under specific-pathogen-free conditions. The University Committee on Use and Care of Animals approved all experiments conducted in this study. *Naip5*$^{-/-}$, *Nlrc4*$^{-/-}$, and *caspase-1*$^{-/-}$ C57BL/6 mice were described previously (9). Although C57BL/6 *caspase-1*$^{-/-}$ mice are also *caspase-11*$^{-/-}$, caspase-11 is expressed poorly in the absence of MAMPs (62) and is not required to activate NLRP3 inflammasomes (63, 64). Therefore, only the relevant *caspase-1*$^{-/-}$ genotype is notated throughout the text and figures.

Mouse bone marrow-derived macrophages. All of the experiments analyzed primary macrophages derived from the bone marrow of mice as described previously (38). On day 6 of culture, unless stated otherwise, macrophages were replated onto coverslips or wells of 24-well plates at a density of 2.5×10^5/well in RPMI 1640 containing 10% fetal bovine serum (RPMI+FBS) and used for experiments within 24 to 48 h.

Bacteria. *L. pneumophila* strain Lp02 (*thyA hsdR rpsL*) is a thymine auxotroph derived from *L. pneumophila* Philadelphia strain 1. Also analyzed were isogenic *dotA* mutants, which are defective for type IV secretion but retain motility, and *flaA* mutants, which lack flagellin but are competent for type IV secretion (8). To induce motility, bacteria were cultured to post-exponential phase (optical density at 600 nm [OD_{600}] of 3.5 to 4.0) on a rotating wheel at 37°C in *N*-(2-acetamido)-2-aminoethanesulfonic acid (ACES; Sigma)-buffered yeast extract broth supplemented with 100 mg/ml thymidine. Because motility enhances bac-

terial entry into macrophages, similar infection levels were achieved by culturing macrophages with three times as many *flaA* mutants as WT *L. pneumophila* organisms.

Intracellular growth. Macrophages were infected with *L. pneumophila* at an MOI of <1 for 2 h; then extracellular bacteria were removed by washing the monolayer three times with RPMI+FBS. At 2 and 72 h, macrophages in duplicate wells were lysed in 1% saponin, and serial dilutions of the lysate were plated in duplicate onto ACES-buffered charcoal-yeast extract agar containing 100 mg/ml thymidine. The fold increase in CFU was calculated as (CFU at 72 h)/(CFU at 2 h).

Microscopy. To quantify delivery of *L. pneumophila* to late endosomes and lysosomes, LAMP-1 was localized by immunofluorescence microscopy. Macrophages infected with WT or *dotA* mutant *L. pneumophila* at an MOI of <1 for 1.5 h were fixed with periodate-lysine-paraformaldehyde fixative containing 5% sucrose (PLP-sucrose) (38) and permeabilized with ice-cold methanol, and then nonspecific binding was blocked by incubation for 5 min with phosphate-buffered saline (PBS) containing 2% heat-inactivated goat serum and 5% sucrose. Cells were then stained using rat anti-LAMP-1 antibody (1:800; Santa Cruz Biotechnologies) and rabbit anti-*Legionella* antibody (1:1,000; kind gift from Ralph Isberg, Tufts University School of Medicine, Boston, MA), followed by Oregon green-conjugated anti-rat and Texas red-conjugated anti-rabbit secondary antibodies (1:1,000; Invitrogen), each incubated for 1 h at 37°C. More than 50 macrophages from triplicate samples were scored for colocalization of LAMP-1 and *L. pneumophila*.

Dispersal of bacteria from the replication vacuole was quantified by microscopy. After incubating macrophages for 1 h with WT or *flaA* mutant *L. pneumophila* at an MOI of <1, extracellular bacteria were washed from the monolayer, and then infected cells were incubated for an additional 17 h. Cultures were fixed, permeabilized, and stained with anti-*Legionella* antibody as described above. At least 100 infected macrophages were analyzed from triplicate samples and recorded as being dispersed if the majority of bacteria were distributed throughout the cell, rather than in one large cluster, as documented previously (8, 35).

Pyroptosis. To quantify pyroptosis, macrophages were infected synchronously with WT or the *flaA* mutant at an MOI of <1 by a 5-min centrifugation at 250 × *g*. After 1 h, extracellular bacteria were removed by washing the monolayers three times with RPMI+FBS. After 7 h, cells were fixed with PLP-sucrose for 30 min at RT. Macrophage nuclei were stained with DAPI before the coverslips were mounted with Pro-long Antifade (Invitrogen). More than 100 macrophages from duplicate samples were examined for the presence of a round, phase-dense nucleus, a hallmark of pyroptosis described previously (5, 8). We verified that macrophages with condensed nuclei had membranes permeabilized by a caspase-1-dependent process, a hallmark of pyroptosis (5). After culture for 1 h in the presence or absence of inhibitors of caspase-1 and/or Atg4, macrophages were infected for 1 h with WT, *flaA*, or *dotA* bacteria. After incubation with propidium iodide (20 μg/ml RPMI) for 20 min at 37°C, cells were rinsed twice with RPMI at 37°C, fixed, and then analyzed by fluorescence microscopy.

The capacity of 100 μM ac-YVAD-cmk to inhibit caspase-1 activity was verified using two assays of pyroptosis (5, 8). C57BL/6J macrophages incubated for 1 h in the presence or absence of the caspase inhibitor were infected with *L. pneumophila* at an MOI of ~50 for 1 h, and then cells were fixed and nuclear morphology analyzed by phase microscopy as described above. Alternatively, macrophages were pretreated with the caspase-1 inhibitor for 1 h and then infected with WT or *flaA* mutant *L. pneumophila* at an MOI of 25 for 1 h. Next, cell-free supernatants were collected from triplicate samples, and the amount of the cytosolic enzyme LDH quantified by the Cytotox96 nonradioactive cytotoxicity assay (Promega). The amount of LDH released after infection with *flaA* mutant or in the presence of YVAD was calculated relative to that released from macrophages infected with WT *L. pneumophila*, which was set to 100%.

Autophagy. Assays that quantify $LC3^+$ puncta in WT and mutant macrophages infected with *L. pneumophila* have a poor signal-to-noise ratio, due to several biological limitations. First, in primary C57BL/6J mouse macrophages derived from bone marrow, autophagosomes mature within ~25 min of formation, as judged by kinetic studies of $LC3^+$ vacuoles (38). A second factor limiting the signal is the low MOI that must be used to avoid pyroptosis. A source of noise is the fact that infections are naturally asynchronous. Therefore, the impact of short, synchronous infection on the autophagy pathway was evaluated using a more sensitive pulse-chase protocol (38). First, a large population of autophagosomes was generated by incubating C57BL/6, *Naip5*$^{-/-}$, *Nlrc4*$^{-/-}$, and *caspase-1*$^{-/-}$ macrophages for 10 to 20 min in Hanks buffer, which lacks amino acids. As a specificity control, macrophages were cultured in RPMI+FBS. Next cells were infected with WT, *dotA*, or *flaA* mutant *L. pneumophila* at an MOI of <3 in Hanks buffer for 15 min. Macrophages were then fixed with PLP-sucrose and permeabilized with methanol, and endogenous LC3 was stained using mouse anti-LC3 antibody (1:100; MBL) and Oregon green-conjugated anti-mouse IgG antibodies (1:150, Invitrogen) as described previously (38). At least 100 macrophages were scored from triplicate samples for the presence of >3 LC3 vacuoles.

To assess the contribution of inflammasome components to the autophagy pathway, C57BL/6, *Naip5*$^{-/-}$, *Nlrc4*$^{-/-}$, and *caspase-1*$^{-/-}$ macrophages were incubated with Hanks buffer for 10 min, and then endogenous LC3 was localized by immunofluorescence microcopy as described above.

To assess the autophagy response to K^+ efflux, macrophages obtained from C57BL/6 mice that carry the GFP-LC3 transgene were incubated with 10 to 50 μM valinomycin (Sigma) in RPMI for 1 h. After fixation with PLP-sucrose and permeabilization with methanol, cells were stained with antibody specific for GFP. As a specificity control, macrophages were instead treated with valinomycin in RPMI supplemented with 150 mM KCl. To inhibit caspase-1 activity, macrophages were pretreated with 100 μM ac-YVAD-cmk (Alexis Biochemicals) for 1 h. At least 100 macrophages per coverslip from triplicate samples were scored for the presence of >3 LC3 vacuoles.

Lipidation to generate LC3II protein was evaluated by Western analysis. C57BL/6 or *caspase-1*$^{-/-}$ macrophages cultured at a density of 10^6 cells/well in a 6-well plate were incubated with 50 to 100 μM valinomycin for 0.5 to 2 h; as a positive control for caspase-1 activation, cells were treated for 2 h with 20 μM nigericin, a more potent K^+ ionophore (Fig. 4). Alternatively, macrophages were treated for 1 h with autophagy inhibitors before culturing for 30 min with either RPMI or Hanks buffer with or without inhibitors (Fig. 5). Next, macrophages were collected in PBS using a cell scraper and then immediately analyzed for the presence of LC3II as described previously (38). Briefly, cells were boiled in Laemmli buffer for 5 min, and then the cell extract was separated using either a 15% or a 15-to-20% gradient SDS-polyacrylamide gel run at 70 V. After proteins were transferred to polyvinylidene difluoride (PVDF) membranes, endogenous LC3II was detected using antibody specific for LC3 (1:500; Novus Biologicals). When macrophages from GFP-LC3 transgenic mice were analyzed, LC3I and LC3II were detected using GFP-specific antibody (1:500; Roche). Bound primary antibodies were visualized using horseradish peroxidase (HRP)-conjugated secondary antibodies (1:4,000; Santa Cruz) and a West Pico chemiluminescence kit (Pierce). To determine if each sample contained similar quantities of protein, membranes were stripped and probed with β-actin-specific antibody (1:4,000; Sigma).

Autophagy was inhibited pharmacologically by two methods. Macrophages were treated with NSC 185058, a synthetic inhibitor of the Atg4 cysteine protease characterized by William Dunn and colleagues (W. Dunn, Jr., D. E. Akin, A. Progulske-Fox, D. A. Ostrov, U.S. patent application US2009/030102) and obtained from the National Cancer Institute's Developmental Therapeutics Program Synthetic Products Repository. The compound was stored as a stock solution (100 mM in dimethyl sulfoxide [DMSO]) at −20°C and diluted 1:2,000 in RPMI+FBS to the concentration desired for experiments. The viability of macrophages treated for 2.5 h with 50 μM of the compound was verified by quantifying

LDH release and propidium iodide staining. Alternatively, macrophages were treated with 10 mM 3-methyladenine (Sigma), a nonspecific inhibitor of class III phosphatidylinositol 3-kinases, including enzymes required for autophagy (37).

Statistical analysis. One-way analysis of variance (ANOVA) followed by Tukey's posttest was used to determine whether means calculated from particular samples were significantly different. A P value of <0.05 was considered statistically significant.

ACKNOWLEDGMENTS

We thank Noboru Mizushima for generating the C57BL/6 GFP-LC3 transgenic mice that were critical to our studies; Russell Vance for *Naip5*$^{-/-}$, *Nlrc4*$^{-/-}$ and *caspase-1*$^{-/-}$ C57BL/6 mouse femurs, insightful discussions, and critical reading of the manuscript; William Dunn for recommendations on use of the Atg4 inhibitor; and Zack Abbott for critical discussions and reading of the manuscript.

Our research was supported by the National Institutes of Health, NIAID (R56 AI076300-01), and the University of Michigan Medical School.

REFERENCES

1. **Eisenberg-Lerner A, Bialik S, Simon HU, Kimchi A.** 2009. Life and death partners: apoptosis, autophagy and the cross-talk between them. Cell Death Differ. **16**:966–975.
2. **Gordy C, He YW.** 2012. The crosstalk between autophagy and apoptosis: where does this lead? Protein Cell. **3**:17–27.
3. **Shen S, Kepp O, Kroemer G.** 2012. The end of autophagic cell death? Autophagy **8**:1–3.
4. **Denton D, Nicolson S, Kumar S.** 2012. Cell death by autophagy: facts and apparent artefacts. Cell Death Differ. **19**:87–95.
5. **Bergsbaken T, Fink SL, Cookson BT.** 2009. Pyroptosis: host cell death and inflammation. Nat. Rev. Microbiol. **7**:99–109.
6. **Zamboni DS, Kobayashi KS, Kohlsdorf T, Ogura Y, Long EM, Vance RE, Kuida K, Mariathasan S, Dixit VM, Flavell RA, Dietrich WF, Roy CR.** 2006. The Birc1e cytosolic pattern-recognition receptor contributes to the detection and control of *Legionella pneumophila* infection. Nat. Immunol. **7**:318–325.
7. **Ren T, Zamboni DS, Roy CR, Dietrich WF, Vance RE.** 2006. Flagellin-deficient Legionella mutants evade caspase-1- and Naip5-mediated macrophage immunity. PLoS Pathog. **2**:e18. http://dx.doi.org/10.1371/journal.ppat.0020018.
8. **Molofsky AB, Byrne BG, Whitfield NN, Madigan CA, Fuse ET, Tateda K, Swanson MS.** 2006. Cytosolic recognition of flagellin by mouse macrophages restricts *Legionella pneumophila* infection. J. Exp. Med. **203**:1093–1104.
9. **Lightfield KL, Persson J, Brubaker SW, Witte CE, von Moltke J, Dunipace EA, Henry T, Sun YH, Cado D, Dietrich WF, Monack DM, Tsolis RM, Vance RE.** 2008. Critical function for Naip5 in inflammasome activation by a conserved carboxy-terminal domain of flagellin. Nat. Immunol. **9**:1171–1178.
10. **Kofoed EM, Vance RE.** 2011. Innate immune recognition of bacterial ligands by NAIPs determines inflammasome specificity. Nature **477**:592–595.
11. **Zhao Y, Yang J, Shi J, Gong YN, Lu Q, Xu H, Liu L, Shao F.** 2011. The NLRC4 inflammasome receptors for bacterial flagellin and type III secretion apparatus. Nature **477**:596–600.
12. **Fink SL, Cookson BT.** 2006. Caspase-1-dependent pore formation during pyroptosis leads to osmotic lysis of infected host macrophages. Cell. Microbiol. **8**:1812–1825.
13. **Silveira TN, Zamboni DS.** 2010. Pore formation triggered by Legionella spp. Is an NLRC4 inflammasome-dependent host cell response that precedes pyroptosis. Infect. Immun. **78**:1403–1413.
14. **Watarai M, Derre I, Kirby J, Growney JD, Dietrich WF, Isberg RR.** 2001. *Legionella pneumophila* is internalized by a macropinocytotic uptake pathway controlled by the Dot/Icm system and the mouse Lgn1 locus. J. Exp. Med. **194**:1081–1096.
15. **Derré I, Isberg RR.** 2004. Macrophages from mice with the restrictive Lgn1 allele exhibit multifactorial resistance to *Legionella pneumophila*. Infect. Immun. **72**:6221–6229.
16. **Amer A, Franchi L, Kanneganti TD, Body-Malapel M, Ozören N, Brady G, Meshinchi S, Jagirdar R, Gewirtz A, Akira S, Núñez G.** 2006. Regulation of *Legionella* phagosome maturation and infection through flagellin and host Ipaf. J. Biol. Chem. **281**:35217–35223.
17. **Fortier A, de Chastellier C, Balor S, Gros P.** 2007. Birc1e/Naip5 rapidly antagonizes modulation of phagosome maturation by *Legionella pneumophila*. Cell. Microbiol. **9**:910–923.
18. **Lamkanfi M, Amer A, Kanneganti TD, Muñoz-Planillo R, Chen G, Vandenabeele P, Fortier A, Gros P, Núñez G.** 2007. The nod-like receptor family member Naip5/Birc1e restricts *Legionella pneumophila* growth independently of caspase-1 activation. J. Immunol. **178**:8022–8027.
19. **Levine B, Mizushima N, Virgin HW.** 2011. Autophagy in immunity and inflammation. Nature **469**:323–335.
20. **Manjithaya R, Subramani S.** 2011. Autophagy: A broad role in unconventional protein secretion? Trends Cell Biol. **21**:67–73.
21. **Duran JM, Anjard C, Stefan C, Loomis WF, Malhotra V.** 2010. Unconventional secretion of Acb1 is mediated by autophagosomes. J. Cell Biol. **188**:527–536.
22. **Taylor MP, Burgon TB, Kirkegaard K, Jackson WT.** 2009. Role of microtubules in extracellular release of poliovirus. J. Virol. **83**:6599–6609.
23. **Takenouchi T, Nakai M, Iwamaru Y, Sugama S, Tsukimoto M, Fujita M, Wei J, Sekigawa A, Sato M, Kojima S, Kitani H, Hashimoto M.** 2009. The activation of P2X7 receptor impairs lysosomal functions and stimulates the release of autophagolysosomes in microglial cells. J. Immunol. **182**:2051–2062.
24. **Starr T, Child R, Wehrly TD, Hansen B, Hwang S, López-Otin C, Virgin HW, Celli J.** 2012. Selective subversion of autophagy complexes facilitates completion of the *Brucella* intracellular cycle. Cell Host Microbe **11**:33–45.
25. **Dupont N, Jiang S, Pilli M, Ornatowski W, Bhattacharya D, Deretic V.** 2011. Autophagy-based unconventional secretory pathway for extracellular delivery of IL-1beta. EMBO J. **30**:4701–4711.
26. **Travassos LH, Carneiro LA, Ramjeet M, Hussey S, Kim YG, Magalhães JG, Yuan L, Soares F, Chea E, Le Bourhis L, Boneca IG, Allaoui A, Jones NL, Nuñez G, Girardin SE, Philpott DJ.** 2010. Nod1 and Nod2 direct autophagy by recruiting ATG16L1 to the plasma membrane at the site of bacterial entry. Nat. Immunol. **11**:55–62.
27. **Billmann-Born S, Lipinski S, Böck J, Till A, Rosenstiel P, Schreiber S.** 2011. The complex interplay of nod-like receptors and the autophagy machinery in the pathophysiology of Crohn disease. Eur. J. Cell Biol. **90**:593–602.
28. **Dupont N, Lacas-Gervais S, Bertout J, Paz I, Freche B, Van Nhieu GT, van der Goot FG, Sansonetti PJ, Lafont F.** 2009. *Shigella* phagocytic vacuolar membrane remnants participate in the cellular response to pathogen invasion and are regulated by autophagy. Cell Host Microbe **6**:137–149.
29. **Suzuki T, Franchi L, Toma C, Ashida H, Ogawa M, Yoshikawa Y, Mimuro H, Inohara N, Sasakawa C, Nuñez G.** 2007. Differential regulation of caspase-1 activation, pyroptosis, and autophagy via Ipaf and ASC in Shigella-infected macrophages. PLoS Pathog. **3**:e111. http://dx.doi.org/10.1371/journal.ppat.0030111.
30. **Amer AO, Swanson MS.** 2005. Autophagy is an immediate macrophage response to *Legionella pneumophila*. Cell. Microbiol. **7**:765–778.
31. **Jounai N, Kobiyama K, Shiina M, Ogata K, Ishii KJ, Takeshita F.** 2011. NLRP4 negatively regulates autophagic processes through an association with Beclin-1. J. Immunol. **186**:1646–1655.
32. **Shi CS, Shenderov K, Huang NN, Kabat J, Abu-Asab M, Fitzgerald KA, Sher A, Kehrl JH.** 2012. Activation of autophagy by inflammatory signals limits IL-β production by targeting ubiquitinated inflammasomes for destruction. Nat. Immunol. **13**:255–263.
33. **Checroun C, Wehrly TD, Fischer ER, Hayes SF, Celli J.** 2006. Autophagy-mediated reentry of *Francisella tularensis* into the endocytic compartment after cytoplasmic replication. Proc. Natl. Acad. Sci. U. S. A. **103**:14578–14583.
34. **Birmingham CL, Smith AC, Bakowski MA, Yoshimori T, Brumell JH.** 2006. Autophagy controls Salmonella infection in response to damage to the Salmonella-containing vacuole. J. Biol. Chem. **281**:11374–11383.
35. **Creasey EA, Isberg RR.** 2012. The protein SdhA maintains the integrity of the Legionella-containing vacuole. Proc. Natl. Acad. Sci. U. S. A. **109**:3481–3486.
36. **Pankiv S, Clausen TH, Lamark T, Brech A, Bruun JA, Outzen H, Øvervatn A, Bjørkøy G, Johansen T.** 2007. P62/sqstm1 binds directly to atg8/lc3 to facilitate degradation of ubiquitinated protein aggregates by autophagy. J. Biol. Chem. **282**:24131–24145.

37. **Klionsky DJ, et al.** 2012. Guidelines for the use and interpretation of assays for monitoring autophagy. Autophagy **8**:445–544.
38. **Swanson MS, Byrne BG, Dubuisson JF.** 2009. Kinetic analysis of autophagosome formation and turnover in primary mouse macrophages. Methods Enzymol. **452**:383–402.
39. **Byrne B, Swanson MS.** 1998. Expression of *Legionella pneumophila* virulence traits in response to growth conditions. Infect. Immun. **66**: 3029–3034.
40. **Ge J, Gong YN, Xu Y, Shao F.** 2012. Preventing bacterial DNA release and absent in melanoma 2 inflammasome activation by a *Legionella* effector functioning in membrane trafficking. Proc. Natl. Acad. Sci. U. S. A. **109**:6193–6198.
41. **Mariathasan S, Monack DM.** 2007. Inflammasome adaptors and sensors: intracellular regulators of infection and inflammation. Nat. Rev. Immunol. **7**:31–40.
42. **Biswas D, Qureshi OS, Lee WY, Croudace JE, Mura M, Lammas DA.** 2008. ATP-induced autophagy is associated with rapid killing of intracellular *Mycobacteria* within human monocytes/macrophages. BMC Immunol. **9**:35.
43. **Damiano JS, Oliveira V, Welsh K, Reed JC.** 2004. Heterotypic interactions among Nacht domains: implications for regulation of innate immune responses. Biochem. J. **381**:213–219.
44. **Hou YC, Chittaranjan S, Barbosa SG, McCall K, Gorski SM.** 2008. Effector caspase Dcp-1 and IAP protein Bruce regulate starvation-induced autophagy during *Drosophila melanogaster* oogenesis. J. Cell Biol. **182**: 1127–1139.
45. **Miao EA, Leaf IA, Treuting PM, Mao DP, Dors M, Sarkar A, Warren SE, Wewers MD, Aderem A.** 2010. Caspase-1-induced pyroptosis is an innate immune effector mechanism against intracellular bacteria. Nat. Immunol. **11**:1136–1142.
46. **Qu Y, Franchi L, Nunez G, Dubyak GR.** 2007. Nonclassical IL-1 beta secretion stimulated by P2X7 receptors is dependent on inflammasome activation and correlated with exosome release in murine macrophages. J. Immunol. **179**:1913–1925.
47. **Keller M, Rüegg A, Werner S, Beer HD.** 2008. Active caspase-1 is a regulator of unconventional protein secretion. Cell **132**:818–831.
48. **Qu Y, Ramachandra L, Mohr S, Franchi L, Harding CV, Nunez G, Dubyak GR.** 2009. P2x7 receptor-stimulated secretion of MHC class II-containing exosomes requires the ASC/NLRP3 inflammasome but is independent of caspase-1. J. Immunol. **182**:5052–5062.
49. **Ramachandra L, Qu Y, Wang Y, Lewis CJ, Cobb BA, Takatsu K, Boom WH, Dubyak GR, Harding CV.** 2010. *Mycobacterium tuberculosis* Synergizes with ATP to induce release of microvesicles and exosomes containing major histocompatibility complex class II molecules capable of antigen presentation. Infect. Immun. **78**:5116–5125.
50. **Bergsbaken T, Fink SL, den Hartigh AB, Loomis WP, Cookson BT.** 2011. Coordinated host responses during pyroptosis: caspase-1-dependent lysosome exocytosis and inflammatory cytokine maturation. J. Immunol. **187**:2748–2754.
51. **Saitoh T, Akira S.** 2010. Regulation of innate immune responses by autophagy-related proteins. J. Cell Biol. **189**:925–935.
52. **Zhou R, Yazdi AS, Menu P, Tschopp J.** 2011. A role for mitochondria in NLRP3 inflammasome activation. Nature **469**:221–225.
53. **Nakahira K, Haspel JA, Rathinam VA, Lee SJ, Dolinay T, Lam HC, Englert JA, Rabinovitch M, Cernadas M, Kim HP, Fitzgerald KA, Ryter SW, Choi AM.** 2011. Autophagy proteins regulate innate immune responses by inhibiting the release of mitochondrial DNA mediated by the NALP3 inflammasome. Nat. Immunol. **12**:222–230.
54. **Saitoh T, Fujita N, Jang MH, Uematsu S, Yang BG, Satoh T, Omori H, Noda T, Yamamoto N, Komatsu M, Tanaka K, Kawai T, Tsujimura T, Takeuchi O, Yoshimori T, Akira S.** 2008. Loss of the autophagy protein ATG16L1 enhances endotoxin-induced IL-1beta production. Nature **456**: 264–268.
55. **Harris J, Hartman M, Roche C, Zeng SG, O'Shea A, Sharp FA, Lambe EM, Creagh EM, Golenbock DT, Tschopp J, Kornfeld H, Fitzgerald KA, Lavelle EC.** 2011. Autophagy controls IL-1beta secretion by targeting pro-IL-1beta for degradation. J. Biol. Chem. **286**:9587–9597.
56. **Kleinnijenhuis J, Oosting M, Plantinga TS, van der Meer JW, Joosten LA, Crevel RV, Netea MG.** 2011. Autophagy modulates the *Mycobacterium tuberculosis*-induced cytokine response. Immunology **134**: 341–348.
57. **Tung SM, Unal C, Ley A, Peña C, Tunggal B, Noegel AA, Krut O, Steinert M, Eichinger L.** 2010. Loss of *Dictyostelium* Atg9 results in a pleiotropic phenotype affecting growth, development, phagocytosis and clearance and replication of *Legionella pneumophila*. Cell. Microbiol. **12**: 765–780.
58. **Matsuda F, Fujii J, Yoshida S.** 2009. Autophagy induced by 2-deoxy-D-glucose suppresses intracellular multiplication of *Legionella pneumophila* in A/J mouse macrophages. Autophagy **5**:484–493.
59. **Joshi AD, Swanson MS.** 2011. Secrets of a successful pathogen: *Legionella* resistance to progression along the autophagic pathway. Front Microbiol. **2**:138.
60. **Choy A, Dancourt J, Mugo B, O'Connor TJ, Isberg RR, Melia TJ, Roy CR.** 2012. The *Legionella* effector RavZ inhibits host autophagy through irreversible Atg8 deconjugation. Science **338**:1072–1076.
61. **Ogawa M, Mimuro H, Yoshikawa Y, Ashida H, Sasakawa C.** 2011. Manipulation of autophagy by bacteria for their own benefit. Microbiol. Immunol. **55**:459–471.
62. **Kang SJ, Wang S, Hara H, Peterson EP, Namura S, Amin-Hanjani S, Huang Z, Srinivasan A, Tomaselli KJ, Thornberry NA, Moskowitz MA, Yuan J.** 2000. Dual role of caspase-11 in mediating activation of caspase-1 and caspase-3 under pathological conditions. J. Cell Biol. **149**:613–622.
63. **Broz P, von Moltke J, Jones JW, Vance RE, Monack DM.** 2010. Differential requirement for caspase-1 autoproteolysis in pathogen-induced cell death and cytokine processing. Cell Host Microbe **8**:471–483.
64. **Kayagaki N, Warming S, Lamkanfi M, Vande Walle L, Louie S, Dong J, Newton K, Qu Y, Liu J, Heldens S, Zhang J, Lee WP, Roose-Girma M, Dixit VM.** 2011. Non-canonical inflammasome activation targets caspase-11. Nature **479**:117–121.